




## Finite-key security analysis of differential-phase-shift quantum key distribution

Akihiro Mizutani <sup>1,2</sup>, Yuki Takeuchi <sup>3</sup>, and Kiyoshi Tamaki <sup>2</sup>

<sup>1</sup>Mitsubishi Electric Corporation, Information Technology R&D Center, 5-1-1 Ofuna, Kamakura-shi, Kanagawa 247-8501, Japan

<sup>2</sup>Faculty of Engineering, University of Toyama, Gofuku 3190, Toyama 930-8555, Japan

<sup>3</sup>NTT Communication Science Laboratories, NTT Corporation, 3-1 Morinosato Wakamiya, Atsugi, Kanagawa 243-0198, Japan



(Received 15 March 2023; accepted 8 May 2023; published 30 May 2023)

Differential-phase-shift (DPS) quantum key distribution (QKD) is one of the major QKD protocols that can be implemented with a simple setup using a laser source and a passive detection unit. Recently, an information-theoretic security proof of this protocol was established by Mizutani *et al.* [[npj Quantum Inf.](#) **5**, 87 (2019)], assuming an infinitely large number of emitted pulses. To implement the DPS protocol in a real-life world, it is indispensable to analyze the security with the finite number of emitted pulses. The extension of the security proof to the finite-size regime requires the accommodation of the statistical fluctuations to determine the amount of privacy amplification. In doing so, Azuma's inequality is often employed, but unfortunately we show that in the case of the DPS protocol, this results in a substantially low key rate. This low key rate is due to a loose estimation of the sum of probabilities regarding three-photon emission whose probability of occurrence is very small. The main contribution of our work is to show that this obstacle can be overcome by exploiting the recently found novel concentration inequality, Kato's inequality. As a result, the key rate of the DPS protocol is drastically improved. For instance, assuming typical experimental parameters, a 3-Mbit secret key can be generated over 77 km for 8.3 hours, which shows the feasibility of DPS QKD under a realistic setup.

DOI: [10.1103/PhysRevResearch.5.023132](https://doi.org/10.1103/PhysRevResearch.5.023132)

### I. INTRODUCTION

Quantum key distribution (QKD) realizes information-theoretically secure communication between two distant parties (Alice and Bob) against any eavesdropper (Eve). Since the first invention of the BB84 protocol [[1](#)], various protocols have been proposed [[2–9](#)]. Among them, the differential-phase-shift (DPS) protocol [[8](#)] is considered to be one of the promising protocols for future QKD implementations. This is because the DPS protocol can be implemented with an experimentally simple setup using a laser source and a passive detection unit. The experimental demonstrations of this protocol have been conducted in Refs. [[10–12](#)] and also its field demonstration has been done in the Tokyo QKD network [[13](#)]. Also, security proofs of the DPS protocol have been intensively studied. In proving the security, the difficulty specific to this protocol is that one needs to deal with a very large Hilbert space since this protocol extracts sifted key information from the phase difference between adjacent pulses, and hence all the emitted pulses are continuously connected like a chain. To simplify the analysis, the previous security proofs have disentangled this chain by introducing a block. This block consists of some emitted pulses, and the protocol extracts only one sifted key bit from each block. For example, the first information-theoretic security proof [[14](#)] assumes that a

single photon exists in each of the blocks. This impractical single-photon assumption has been mitigated to a blockwise phase-randomized coherent source in Refs. [[15,16](#)]. Applying a random phase shift to each block enables one to analyze the security for each photon number emission event separately. The recent work [[17](#)] has removed the need of the block-wise phase randomization and proven the security under simplified source assumptions including the case with two phase-modulated coherent states. Furthermore, the security proof in Ref. [[18](#)] has extended the one in Ref. [[17](#)] to cover the case where the source emits any two identical and independent states. Importantly, these works [[14–18](#)] guarantee the information-theoretic security of the DPS protocol, namely, these proofs are valid under any of Eve's attack. Also, a recent work [[19](#)] has studied the performance of the DPS protocol by assuming a specific Eve's attack in the satellite environment.

The information-theoretic security proofs of the DPS protocol so far are only valid in the asymptotic regime, where the length of the sifted key is assumed to be infinite. Like other major QKD protocols [[20–26](#)], it is indispensable to reveal its key-generation efficiency with the finite-key length to implement the DPS protocol in real-life environments. In the finite-key analysis, it is crucial to evaluate statistical deviation terms of concentration inequalities in deriving an upper bound on the amount of privacy amplification. In so doing, it is important to employ an inequality that results in a small deviation with a smaller number of trials; otherwise, the speed of convergence to the asymptotic key rate becomes slow, leading to a poor performance.

In this paper, we extend our previous information-theoretic security proof [[17](#)] of the DPS protocol to the finite-size

Published by the American Physical Society under the terms of the [Creative Commons Attribution 4.0 International license](#). Further distribution of this work must maintain attribution to the author(s) and the published article's title, journal citation, and DOI.

one. As implied in the previous work [17], this extension can be achieved by using Azuma's inequality [27] to deal with correlated random variables. This inequality is a well-known concentration inequality used in various security proofs [21,22,28–31]. Unfortunately, however, we reveal that the analysis with Azuma's inequality results in a substantially low key rate under a realistic experimental setup. To overcome this problem, we exploit Kato's inequality [32], which is a novel concentration inequality, and show that the key rate is drastically improved. More concretely, our numerical simulation shows that its achievable distance becomes more than three times longer than the one based on the analysis using Azuma's inequality (see Fig. 5). Note that using Kato's inequality instead of Azuma's one gives a significant improvement in the key rate only if the estimation of the leaked information involves events that occur with very small probability. This was pointed out in the recent finite-key analyses [20,33] of the twin-field QKD protocol. In our case, such a rare event is a detection event originating from emissions of three photons, and we show that its probability is small enough to enjoy significant improvement with the use of Kato's inequality. We explain its details in Sec. IV C.

The rest of the paper is structured as follows. Section II explains the assumptions we impose on the users' devices. We describe our DPS protocol in Sec. III and prove its security in Sec. IV. Section V presents the numerical simulation results of the key rate. In Sec. VI, we compare the key rates obtainable using the analysis based on Kato's and Azuma's inequalities. Finally, Sec. VII concludes our paper.

## II. ASSUMPTIONS ON DEVICES

Before describing the protocol, we summarize the assumptions we make on the source and measurement units. These are the same as those in our previous work [17], but we describe them for the completeness of this paper. In this paper, we consider that Alice employs three pulses contained in a single block, and Alice and Bob try to extract a key bit from each block.

### A. Assumptions on Alice's source unit

First, we list up the assumptions on Alice's source as follows:

(A1) Alice randomly chooses a three-bit sequence  $\mathbf{b}_A := b_A^{(1)}b_A^{(2)}b_A^{(3)} \in \{0, 1\}^3$ , where bit  $b_A^{(u)}$  is encoded only on the  $u$ th emitted pulse of system  $S_u$ . Depending on the chosen  $\mathbf{b}_A$ , Alice prepares the following three-pulse state of systems  $\mathbf{S} := S_1S_2S_3$ :

$$\hat{\rho}_{\mathbf{S}}^{\mathbf{b}_A} := \bigotimes_{u=1}^3 \hat{\rho}_{S_u}^{b_A^{(u)}}. \quad (1)$$

Here,  $\hat{\rho}_{S_u}^{b_A^{(u)}}$  is a density operator of the  $u$ th pulse when  $b_A^{(u)}$  is selected. We assume that the purified system  $R_u$  of  $\hat{\rho}_{S_u}^{b_A^{(u)}}$  is possessed by Alice, and Eve cannot access system  $R_u$ . Note that state  $\hat{\rho}_{S_u}^{b_A^{(u)}}$  is allowed to be different for each system  $S_u$ .

(A2) The probability of the  $u$ th emitted pulse being the vacuum state is independent of bit  $b_A^{(u)}$ . That is,

$$\text{tr}[|\text{vac}\rangle\langle\text{vac}|\hat{\rho}_{S_u}^0] = \text{tr}[|\text{vac}\rangle\langle\text{vac}|\hat{\rho}_{S_u}^1] \quad (2)$$

holds for any  $u$ , where  $|\text{vac}\rangle$  denotes the vacuum state.

(A3) For any chosen bit sequence  $\mathbf{b}_A$ , the probability that any single block of pulses contains  $n$  ( $n \in \{1, 2, 3\}$ ) or more photons is upper-bounded by  $q_n$ ,

$$\sum_{m \geq n} \text{tr}[|m\rangle\langle m|\hat{\rho}_{\mathbf{S}}^{\mathbf{b}_A}] \leq q_n, \quad (3)$$

where  $|m\rangle$  denotes the photon-number state in all the optical modes.

Importantly, we do not assume blockwise phase randomization as in Refs. [15,16]. Note that such randomization enables us to regard the state of every single block as a classical mixture of the Fock states. However, our security proof holds without such an assumption and is valid even if there exists a phase coherence among the emitted blocks. This allows us to employ the source assumed in the original DPS protocol [7], which emits a pulse in a coherent state randomly chosen from  $\{|\alpha\rangle, |-\alpha\rangle\}$ .

We remark that Ref. [18] has mitigated assumption (A2) to cover the case where Alice only knows the range of the probabilities of being the vacuum state. It could be possible to prove the security of the DPS protocol with this mitigated assumption in the finite-size regime, but for simplicity of discussion we adopt the above assumptions based on Ref. [17].

### B. Assumptions on Bob's measurement unit

Next we explain the assumptions on Bob's measurement unit.

(B1) Bob measures incoming pulses using a one-bit delay Mach-Zehnder interferometer with 50:50 beam splitters (BSs). This delay is equal to the time interval of the neighboring emitted pulses.

(B2) The interfered pulses are detected by two photon-number-resolving (PNR) detectors, which discriminate the vacuum, a single photon, and two or more photons in a specific optical mode. We assume that the quantum efficiencies and dark countings are the same for both detectors. According to which PNR detector reports a click, Bob obtains a raw key bit  $d \in \{0, 1\}$ .

For each incoming block, the  $j$ th ( $j \in \{1, 2\}$ ) time slot is defined by the expected detection time where the  $j$ th and  $(j+1)$ th incoming pulses interfere. Also, the zeroth and third time slots are defined by the expected detection time where the first (third) incoming pulse and third (first) one in the previous (next) block interfere.

## III. ACTUAL PROTOCOL

We describe our DPS protocol, which is the finite-size version of our previous protocol [17]. In its description,  $\text{wt}(\mathbf{b})$  denotes the number of 1's in a bit string  $\mathbf{b}$ . We depict a schematic diagram of our DPS protocol in Fig. 1.

(P1) Alice and Bob, respectively, repeat the following procedures for  $N_{\text{em}}$  rounds:

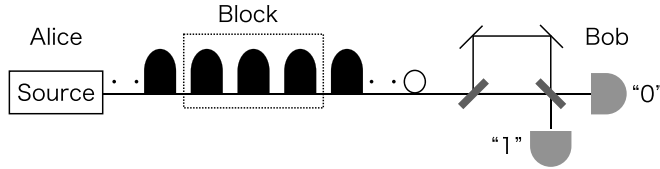


FIG. 1. Schematics for our DPS protocol. Alice sends blocks of three pulses to Bob and he receives them with the one-bit delay Mach-Zehnder interferometer and detectors.

(a) Alice generates uniformly random three bits  $\mathbf{b}_A \in \{0, 1\}^3$  and sends three pulses in state  $\hat{\rho}_S^{\mathbf{b}_A}$  to Bob via a quantum channel.

(b) Bob forwards the incoming three pulses into the Mach-Zehnder interferometer followed by photon detection by the PNR detectors. We call the round *detected* if Bob detects exactly one photon in total among the first and second time slots. The detection event at the  $j$ th ( $j \in \{1, 2\}$ ) time slot determines the raw key bit  $d \in \{0, 1\}$ , depending on which of the two detectors clicks.

(P2) Bob takes note of a set of detected rounds  $\mathcal{D} \subseteq \{1, \dots, N_{\text{em}}\}$  with length  $N_{\text{det}} := |\mathcal{D}|$ , a set of time slots  $\mathbf{j} := (j_i)_{i \in \mathcal{D}}$ , and a raw key  $\mathbf{d} := (d_i)_{i \in \mathcal{D}}$ . Here,  $j_i$  and  $d_i$  are  $j$  and  $d$  of the  $i$ th detected round, respectively. Bob associates each detected round with a *code* or *sample* round with probability  $t$  or  $1 - t$ , respectively, with  $0 < t < 1$ . He defines the code set  $\mathcal{D}_{\text{code}}$  with length  $N_{\text{code}} := |\mathcal{D}_{\text{code}}|$ , the sample one  $\mathcal{D}_{\text{samp}} := \mathcal{D} \setminus \mathcal{D}_{\text{code}}$  with length  $N_{\text{samp}} := |\mathcal{D}_{\text{samp}}|$ , his sifted key  $\kappa_B := (d_i)_{i \in \mathcal{D}_{\text{code}}}$ , and the sample sequence  $\kappa_B^{\text{samp}} := (d_i)_{i \in \mathcal{D}_{\text{samp}}}$ .

(P3) Bob announces  $\mathcal{D}_{\text{code}}$ ,  $\mathcal{D}_{\text{samp}}$ ,  $\mathbf{j}$ , and  $\kappa_B^{\text{samp}}$  to Alice through an authenticated public channel.

(P4) Alice calculates her sifted key  $\kappa_A := (b_A^{(j_i)} \oplus b_A^{(j_i+1)})_{i \in \mathcal{D}_{\text{code}}}$  and sample sequence  $\kappa_A^{\text{samp}} := (b_A^{(j_i)} \oplus b_A^{(j_i+1)})_{i \in \mathcal{D}_{\text{samp}}}$ .

(P5) (Bit error correction.) Alice estimates the bit error rate in the code rounds using the information of the one in the sample rounds. Depending on the estimated error rate, Alice chooses and announces a bit error correcting code and sends syndrome information on her sifted key  $\kappa_A$  by consuming a preshared secret key of length  $N_{\text{EC}}$ . Bob corrects the bit errors in his sifted key  $\kappa_B$  and obtains the reconciled key  $\kappa_B^{\text{rec}}$ . By consuming a preshared secret key of length  $\zeta'$ , Alice and Bob verify the correctness of their resulting reconciled keys by comparing the output ( $\zeta'$  bit) of a randomly chosen universal<sub>2</sub> hash function  $H_{\text{EC}}$ .

(P6) (Privacy amplification.) Alice and Bob conduct privacy amplification by shortening  $N_{\text{PA}}$  bits to, respectively, share the final keys  $k_A$  and  $k_B$  of length

$$N_{\text{fin}} = N_{\text{code}} - N_{\text{PA}}. \quad (4)$$

We define two parameters which will be used in our security proof in Sec. IV C. We define the detection rate by

$$0 \leq Q := \frac{N_{\text{det}}}{N_{\text{em}}} \leq 1 \quad (5)$$

and the bit error rate in the sample rounds by

$$e_{\text{bit}} := \frac{\text{wt}(\kappa_A^{\text{samp}} \oplus \kappa_B^{\text{samp}})}{N_{\text{samp}}}. \quad (6)$$

The net length of the final key, namely, the increased length of the secret key is written as

$$\ell = N_{\text{fin}} - N_{\text{EC}} - \zeta'. \quad (7)$$

#### IV. SECURITY PROOF

In this section, we prove the security of the actual protocol described in Sec. III in the finite-size regime. In Sec. IV A, we explain in what sense we claim that the protocol is secure. Here, we adopt the universal composable security criterion [34], which is widely used in the security proofs of QKD. In Sec. IV B, we prove the security of the actual protocol based on the complementarity argument [35]. This argument reduces the security proof to estimating how well Alice can predict the outcome of the complementary observable, which is quantified by the number of phase errors. In Sec. IV C, we estimate the upper bound on the number of phase errors and leave its detailed statistical analysis to Appendix C. Note that another security proof framework based on the entropic uncertainty principle [36] and the leftover hashing lemma [37] also reduces the proof to estimating the upper bound on the number of phase errors [25,26]. Hence, using the discussions in Sec. IV C, we can also prove the security within this framework.

We summarize the definitions used in this section. The projector is defined by  $\hat{P}[|x\rangle] := |x\rangle\langle x|$ , the 1-norm  $\|\hat{A}\|_1$  for linear operator  $\hat{A}$  by  $\|\hat{A}\|_1 := \text{tr}\sqrt{\hat{A}^\dagger \hat{A}}$ , and function  $h(x)$  by

$$h(x) := \begin{cases} -x \log_2 x - (1-x) \log_2 (1-x) & (0 \leq x \leq 1/2) \\ 1 & (x > 1/2). \end{cases} \quad (8)$$

The Kronecker delta is defined by  $\delta_{x,y} = 1$  if  $x = y$  and  $\delta_{x,y} = 0$  otherwise.

##### A. Security criterion

Here, we explain our security criterion that satisfies the universal composable security [34]. When the length of the final key is  $N_{\text{fin}}$ , we denote the state of Alice's and Bob's final keys and Eve's quantum system by

$$\hat{\rho}_{ABE|N_{\text{fin}}}^{\text{fin}} := \sum_{\substack{k_A, k_B \in \\ \{0, 1\}^{N_{\text{fin}}}}} \text{Pr}[k_A, k_B | N_{\text{fin}}] |k_A, k_B\rangle\langle k_A, k_B|_{AB} \otimes \hat{\rho}_{E|N_{\text{fin}}}^{\text{fin}}(k_A, k_B) \quad (9)$$

and denote the one of the ideal final keys and Eve's quantum system by

$$\hat{\rho}_{ABE|N_{\text{fin}}}^{\text{ideal}} := \frac{1}{2^{N_{\text{fin}}}} \sum_{k \in \{0, 1\}^{N_{\text{fin}}}} |k, k\rangle\langle k, k|_{AB} \otimes \text{tr}_{AB}(\hat{\rho}_{ABE|N_{\text{fin}}}^{\text{fin}}). \quad (10)$$

We say a protocol is  $\epsilon_{\text{sec}}$ -secure if

$$\frac{1}{2} \sum_{N_{\text{fin}} \geq 0} \text{Pr}[N_{\text{fin}}] \|\hat{\rho}_{ABE|N_{\text{fin}}}^{\text{ideal}} - \hat{\rho}_{ABE|N_{\text{fin}}}^{\text{fin}}\|_1 \leq \epsilon_{\text{sec}}. \quad (11)$$

Here,  $\text{Pr}[N_{\text{fin}}]$  denotes the probability of obtaining the final key of length  $N_{\text{fin}}$  by executing the protocol, where aborting

the protocol corresponds to  $N_{\text{fin}} = 0$ . We say the protocol is  $\epsilon_c$ -correct if

$$\sum_{N_{\text{fin}} \geq 0} \Pr[N_{\text{fin}}] \Pr[k_A \neq k_B | N_{\text{fin}}] \leq \epsilon_c. \quad (12)$$

Also, we say the protocol is  $\epsilon_s$ -secret if

$$\frac{1}{2} \sum_{N_{\text{fin}} \geq 0} \Pr[N_{\text{fin}}] \|\hat{\rho}_{AE|N_{\text{fin}}}^{\text{fin}} - \hat{\rho}_{AE|N_{\text{fin}}}^{\text{ideal}}\|_1 \leq \epsilon_s. \quad (13)$$

Here, we define

$$\hat{\rho}_{AE|N_{\text{fin}}}^{\text{fin}} := \text{tr}_B[\hat{\rho}_{ABE|N_{\text{fin}}}^{\text{fin}}] \quad (14)$$

and

$$\hat{\rho}_{AE|N_{\text{fin}}}^{\text{ideal}} := \text{tr}_B[\hat{\rho}_{ABE|N_{\text{fin}}}^{\text{ideal}}]. \quad (15)$$

As shown in Ref. [35], if the protocol is  $\epsilon_c$ -correct and  $\epsilon_s$ -secret, it is  $\epsilon_{\text{sec}}$ -secure with

$$\epsilon_{\text{sec}} = \epsilon_c + \epsilon_s. \quad (16)$$

For completeness of this paper, we give the proof of Eq. (16) in Appendix A.

As for correctness, due to the verification of the error correction executed in step (P5), the probability of obtaining different final keys is upper-bounded by  $2^{-\zeta'}$  [26]. We state this as the following theorem, whose proof is given in Appendix B.

*Theorem 1.* (Correctness.) The actual protocol described in Sec. III is  $\epsilon_c$ -correct with  $\epsilon_c = 2^{-\zeta'}$ .

In the following Secs. IV B and IV C, our purpose is to derive the secrecy parameter defined in Eq. (13).

### B. Derivation of secrecy parameter

Here, we derive the upper bound on the secrecy parameter  $\epsilon_s$  in Eq. (13). In so doing, we consider virtual procedures equivalent to Alice's state preparation in step (P1)a, the calculation of her sifted key  $\kappa_A$  and sample sequence  $\kappa_A^{\text{samp}}$  in step (P4), and Bob's measurements. These procedures simplify the derivation of  $\epsilon_s$  and the final state  $\hat{\rho}_{AE|N_{\text{fin}}}^{\text{fin}}$  of Alice's and Eve's systems is the same as the one of the actual protocol. As can be seen from Eq. (13), Bob's system does not appear in the definition of the  $\epsilon_s$ -secret. Hence, we can consider that Bob virtually executes an operation such that it makes it easier to prove Eq. (13). These virtual procedures are the same as those in our previous work [17], and we concisely state them below.

As for the virtual procedure equivalent to step (P1)a, Alice prepares three auxiliary qubits of systems  $A := A_1 A_2 A_3$ , generates state

$$|\Phi\rangle_{ASR} := 2^{-3/2} \bigotimes_{u=1}^3 \sum_{b_A^{(u)}=0,1} \hat{H} |b_A^{(u)}\rangle_{A_u} |\psi_{b_A^{(u)}}\rangle_{S_u R_u} \quad (17)$$

and sends system  $S$  to Bob. Here,  $\hat{H} := 1/\sqrt{2} \sum_{x,y=0,1} (-1)^{xy} |x\rangle\langle y|$ ,  $\mathbf{R} := R_1 R_2 R_3$ , and  $|\psi_{b_A^{(u)}}\rangle_{S_u R_u}$  is a purification of  $\hat{\rho}_{S_u}^{b_A^{(u)}}$ .

Regarding the virtual procedure for step (P4), Alice calculates bit  $b_A^{(j)} \oplus b_A^{(j+1)}$  by applying controlled-not (CNOT) gate  $\hat{U}_{\text{CNOT}}^{(j)}$  with  $\hat{U}_{\text{CNOT}}^{(j)} |x\rangle_{A_j} |y\rangle_{A_{j+1}} := |x\rangle_{A_j} |x \oplus y\rangle_{A_{j+1}}$  for  $x, y \in$

$\{0, 1\}$  followed by measuring system  $A_j$  in the  $X$  basis. Here, we define  $Z$ - and  $X$ -basis states as  $\{|0\rangle, |1\rangle\}$  and  $\{|+\rangle, |-\rangle\}$  with  $|\pm\rangle := (|0\rangle \pm |1\rangle)/\sqrt{2}$ , respectively.

In the complementary argument [35], we are interested in how well Alice can predict the outcome  $z_j \in \{0, 1\}$  if system  $A_j$  were measured in the  $Z$  basis, which is the complementary basis of the key generation basis (namely, the  $X$  basis). Here, we define  $z_j$  as the  $Z$ -basis measurement outcome of system  $A_j$  before performing  $\hat{U}_{\text{CNOT}}^{(j)}$ . As for  $z_j$ , since  $\hat{U}_{\text{CNOT}}^{(j)}$  and  $Z$ -basis measurement of system  $A_j$  commute,  $z_j$  is regarded as the outcome of the same measurement after performing  $\hat{U}_{\text{CNOT}}^{(j)}$ . Bob's role is to help Alice's prediction of  $z_j$ . In particular, instead of Bob learning the key bit by interfering with the  $j$ th and  $(j+1)$ th pulses, he measures which of the two pulses contains a single photon, whose information is sent to Alice. Also, to predict  $z_j$ , Alice measures her system  $A_{j+1}$  in the  $Z$  basis after performing  $\hat{U}_{\text{CNOT}}^{(j)}$ . This gives Alice the information of the outcome  $z_j \oplus z_{j+1}$ . Note that this prediction strategy using Alice's and Bob's information is the same as the one of our previous analysis [17]. We define the occurrence of a *phase error* if her prediction fails. More precisely, Alice's task is to predict the  $Z$ -basis measurement outcomes  $\mathbf{z}_{\text{code}} := (z_j)_{j \in \mathcal{D}_{\text{code}}}$  by using the information sent by Bob and Alice's information of  $z_j \oplus z_{j+1}$  when the auxiliary qubits of systems  $A_{\text{code}} := (A_j)_{j \in \mathcal{D}_{\text{code}}}$  were measured in the  $Z$  basis just after Bob completes all the detections. We denote the prediction of  $\mathbf{z}_{\text{code}}$  by  $\mathbf{z}_{\text{code}}^*$ . Then, the complementarity argument [35,38] claims that if  $\mathbf{z}_{\text{code}} \oplus \mathbf{z}_{\text{code}}^*$  is in a set  $\mathcal{T}_{\text{ph}} \subset \{0, 1\}^{N_{\text{code}}}$  with unit probability, by shortening the reconciled key by

$$N_{\text{PA}} = \log_2 |\mathcal{T}_{\text{ph}}| + \zeta \quad (18)$$

for  $\zeta > 0$  in the privacy amplification step (P6), we obtain  $\epsilon_s = \sqrt{2} \sqrt{2^{-\zeta}}$ . If  $\mathbf{z}_{\text{code}} \oplus \mathbf{z}_{\text{code}}^*$  is not in  $\mathcal{T}_{\text{ph}}$  with probability  $\epsilon$ , namely,

$$\Pr[\mathbf{z}_{\text{code}} \oplus \mathbf{z}_{\text{code}}^* \notin \mathcal{T}_{\text{ph}}] \leq \epsilon, \quad (19)$$

we have  $\epsilon_s = \sqrt{2} \sqrt{\epsilon + 2^{-\zeta}}$  [35,38]. One way to obtain Eq. (19) is to estimate the upper bound on the number  $N_{\text{ph}}$  of phase errors. That is, if we have

$$\Pr[N_{\text{ph}} > N_{\text{ph}}^U] \leq \epsilon \quad (20)$$

with  $N_{\text{ph}}^U$  being a function of experimentally available data, we obtain Eq. (19). This is simply because  $N_{\text{ph}} \leq N_{\text{ph}}^U$  leads to  $\mathbf{z}_{\text{code}} \oplus \mathbf{z}_{\text{code}}^* \in \mathcal{T}_{\text{ph}}$  by setting  $\mathcal{T}_{\text{ph}} = \{\mathbf{b} \in \{0, 1\}^{N_{\text{code}}} | \text{wt}(\mathbf{b}) \leq N_{\text{ph}}^U\}$ , whose number of elements  $|\mathcal{T}_{\text{ph}}|$  is upper bounded by  $2^{N_{\text{code}} h(N_{\text{ph}}^U/N_{\text{code}})}$  with  $h(x)$  defined in Eq. (8). We summarize the arguments in this section as the following theorem.

*Theorem 2.* (Secrecy.) For the protocol described in Sec. III, if the number of phase errors  $N_{\text{ph}}$  satisfies the following regardless of Eve's attack:

$$\Pr[N_{\text{ph}} > N_{\text{ph}}^U] \leq \epsilon \quad (21)$$

for  $\epsilon$  ( $0 \leq \epsilon \leq 1$ ) and  $N_{\text{ph}}^U$  being a function of experimentally available data, and if the amount of privacy amplification  $N_{\text{PA}}$  is set to be

$$N_{\text{PA}} = N_{\text{code}} h\left(\frac{N_{\text{ph}}^U}{N_{\text{code}}}\right) + \zeta \quad (22)$$

for  $\zeta > 0$ , the protocol is  $\epsilon_s$ -secret with

$$\epsilon_s = \sqrt{2}\sqrt{\epsilon + 2^{-\zeta}}. \quad (23)$$

By combining Eqs. (7) and (16), and Theorems 1 and 2, we obtain the following corollary.

*Corollary 1.* For any  $\zeta, \zeta' > 0$  and under Eq. (21), the protocol described in Sec. III generates the secret key of length

$$\ell = N_{\text{code}} \left[ 1 - h \left( \frac{N_{\text{ph}}^{\text{U}}}{N_{\text{code}}} \right) \right] - \zeta - N_{\text{EC}} - \zeta' \quad (24)$$

with  $\epsilon_{\text{sec}} = 2^{-\zeta'} + \sqrt{2}\sqrt{\epsilon + 2^{-\zeta}}$ -secure.

To complete our security proof, the remaining task is to derive the upper bound  $N_{\text{ph}}^{\text{U}}$  as well as the failure probability  $\epsilon$  of the estimation in Eq. (21). Note that  $N_{\text{ph}}^{\text{U}}$  is a function of the parameter  $q_n$ , which characterizes the source, as well as of random variables, such as  $N_{\text{em}}, N_{\text{det}}, N_{\text{code}}, N_{\text{samp}}$ , and  $e_{\text{bit}}$ , all of which are actually observed in the experiment.

### C. Estimation of the number of phase errors and its failure probability

In this section, we derive the upper bound on the number of phase errors and the failure probability of its estimation. The result in this section is an extension of our previous Theorem 1 in Ref. [17] to the finite-size regime.

We aim to estimate the number of phase errors in the code rounds using experimentally observed numbers. In so doing, we define POVM (positive operator valued measure) elements for obtaining the phase error event in the code round and the bit error event in the sample round. To define these POVMs, we introduce the POVM element for Bob's detected event. Given Bob obtains the detected event, POVM elements  $\{\hat{\Pi}_{j,d}\}_{j,d}$  for detecting bit  $d \in \{0, 1\}$  at the  $j$ th ( $j \in \{1, 2\}$ ) time slot can be written as [17]

$$\hat{\Pi}_{j,d} := \hat{P}[\hat{\Pi}_{j,d} \rangle_B], \quad (25)$$

with

$$|\hat{\Pi}_{j,d} \rangle_B := \frac{\sqrt{w_j} |j \rangle_B + (-1)^d \sqrt{w_{j+1}} |j+1 \rangle_B}{\sqrt{2}}, \quad (26)$$

where  $w_1 = w_3 = 1$  and  $w_2 = 1/2$ . Here,  $\{|i \rangle_B\}_{i=1}^3$  denotes the orthogonal states, where  $|2 \rangle_B$  represents that the second incoming pulse has a single photon, and  $|1 \rangle_B$  ( $|3 \rangle_B$ ) represents that the first pulse passing the long arm (third pulse passing the short arm) of the first BS in the Mach-Zehnder interferometer contains a single photon. As explained in Sec. IV B, the phase error event occurs when Alice fails the prediction of the Z-basis measurement outcome  $z_j$  of system  $A_j$ . The explicit formula of POVM element  $\hat{e}_{\text{ph}}$  corresponding to obtaining the phase error event is the same as our previous work [17], which is given by

$$\hat{e}_{\text{ph}} = \sum_{j=1}^2 \sum_z \hat{P}[|z \rangle_A] \otimes [w_j \delta_{z_{j+1}, 1} \hat{P}[|j \rangle_B] + w_{j+1} \delta_{z_j, 1} \hat{P}[|j+1 \rangle_B]] \quad (27)$$

with  $\mathbf{z} := z_1 z_2 z_3 \in \{0, 1\}^3$ . Since  $\hat{e}_{\text{ph}}$  is diagonal in the basis  $|z \rangle_A$ , the measurement of the weight  $a := \text{wt}(\mathbf{z})$ , namely,

$\{\hat{P}_a\}_{a \in \{0,1,2,3\}}$  with

$$\hat{P}_a := \sum_{\mathbf{z}: \text{wt}(\mathbf{z})=a} \hat{P}[|z \rangle_A] \quad (28)$$

and  $\{\hat{e}_{\text{ph}}, I_{AB} - \hat{e}_{\text{ph}}\}$  commute. To relate the probability of obtaining a phase error with the one of a bit error, we also introduce the POVM element  $\hat{e}_{\text{bit}}$  corresponding to obtaining a bit error. This is given by [17]

$$\hat{e}_{\text{bit}} = \sum_{j=1}^2 [(\hat{P}[|++ \rangle_{A_j A_{j+1}}] + \hat{P}[|-- \rangle_{A_j A_{j+1}}]) \otimes \hat{\Pi}_{j,1} + (\hat{P}[|+- \rangle_{A_j A_{j+1}}] + \hat{P}[|-+ \rangle_{A_j A_{j+1}}]) \otimes \hat{\Pi}_{j,0}]. \quad (29)$$

Then, thanks to Lemmas 1 and 2 in Ref. [17], we have the relation between the probabilities of obtaining a phase error, a bit error, and the weight  $a$  as

$$\text{tr}[\hat{e}_{\text{ph}} \hat{\sigma}_{AB}] \leq \lambda (\text{tr}[\hat{e}_{\text{bit}} \hat{\sigma}_{AB}] + \sqrt{\text{tr}[\hat{\sigma}_{AB} \hat{P}_1] \cdot \text{tr}[\hat{\sigma}_{AB} \hat{P}_3]}) + \sum_{a=2,3} \text{tr}[\hat{\sigma}_{AB} \hat{P}_a], \quad (30)$$

with  $\lambda := 3 + \sqrt{5}$ . Importantly, this inequality holds for any state  $\hat{\sigma}_{AB}$  of systems  $AB$ .

To derive the upper bound on the number of phase errors  $N_{\text{ph}}^{\text{U}}$ , we consider the following stochastic trial of measuring  $N_{\text{det}}$  systems  $AB$ . As described in step (P2) of the actual protocol, Bob probabilistically associates each detected round with the code or sample one with probability  $t$  or  $1-t$ , respectively. For the code rounds, Alice and Bob extract the secret key while the sample ones are used to learn bit error rate  $e_{\text{bit}}$  defined in Eq. (6). We define the random variable  $\chi_r^{(i)} \in \{0, 1\}$ , which takes the value of 0 (1) if the  $i$ th detected round with  $i \in \mathcal{D}$  is the code (sample) one. If  $\chi_r^{(i)} = 0$ , Alice carries out the quantum nondemolition (QND) measurement on her three qubits associated with the  $i$ th detected round to learn the weight  $\text{wt}(\mathbf{z})$  with the POVM  $\{\hat{P}_a\}_{a=0}^3$  defined in Eq. (28). After that, Alice and Bob measure their systems to know whether the  $i$ th detected round has a phase error or not by the POVM  $\{\hat{e}_{\text{ph}}, I_{AB} - \hat{e}_{\text{ph}}\}$  defined in Eq. (27). Recall that such simultaneous measurements are allowed because  $\hat{e}_{\text{ph}}$  and  $\hat{P}_a$  commute for any  $a \in \{0, 1, 2, 3\}$ . Figure 2 depicts Alice's measurement procedures when  $\chi_r^{(i)} = 0$ . On the other hand, if  $\chi_r^{(i)} = 1$ , Alice and Bob measure their systems to know whether the  $i$ th detected round has a bit error or not by the POVM  $\{\hat{e}_{\text{bit}}, I_{AB} - \hat{e}_{\text{bit}}\}$  defined in Eq. (29). These situations are illustrated in Fig. 3.

In this stochastic trial, the  $i$ th measurement outcome is in set

$$\mathcal{S} := \bigcup_{a=0}^3 \{\text{ph} \wedge a, \overline{\text{ph}} \wedge a\} \cup \{\text{bit}, \overline{\text{bit}}\}, \quad (31)$$

where ph (bit) denotes the measurement outcome that the  $i$ th detected round entails the phase (bit) error, and  $\overline{\text{ph}}$  ( $\overline{\text{bit}}$ ) has no-phase (no-bit) error. We introduce the following random variables  $\chi_{\text{ph}}^{(i)}, \{\chi_a^{(i)}\}_{a=0}^3$  and  $\chi_{\text{bit}}^{(i)}$ , each of which takes the value of 0 or 1 according to the  $i$ th measurement outcome:

$$\chi_{\text{ph}}^{(i)} = \begin{cases} 1 & \text{if the } i\text{th measurement outcome is ph} \\ 0 & \text{otherwise,} \end{cases} \quad (32)$$

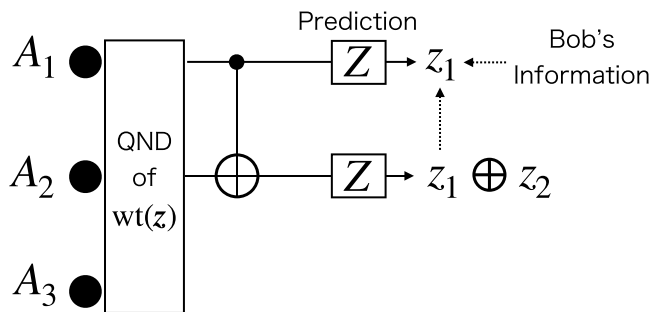


FIG. 2. Schematics of Alice’s measurement procedures for  $j = 1$  when  $\chi_r^{(i)} = 0$ , i.e., the code rounds. She first carries out the QND measurement to learn the weight  $\text{wt}(z)$  followed by performing the CNOT gate, and using the information of  $z_1 \oplus z_2$  and the one sent by Bob, Alice predicts the outcome  $z_1$ . Recall that the phase error event is the one if this prediction fails.

$$\chi_a^{(i)} = \begin{cases} 1 & \text{if the } i\text{th measurement outcome is } a \\ 0 & \text{otherwise,} \end{cases} \quad (33)$$

and

$$\chi_{\text{bit}}^{(i)} = \begin{cases} 1 & \text{if the } i\text{th measurement outcome is bit} \\ 0 & \text{otherwise.} \end{cases} \quad (34)$$

We also introduce  $\{F^{(i)}\}_{i=0}^{N_{\text{det}}}$  as the filtration with  $F^{(i)}$  identifying the random variables including  $\chi_{\text{ph}}^{(i)}$ ,  $\{\chi_a^{(i)}\}_{a=0}^3$  and  $\chi_{\text{bit}}^{(i)}$  for  $i' \in \{1, 2, \dots, i\}$ . That is,  $F^{(i)} \subseteq 2^\Omega$  is a  $\sigma$  algebra on sample space  $\Omega = \mathcal{S}^{\times N_{\text{det}}}$ , which satisfies  $F^{(i)} \subseteq F^{(j)}$  and  $E[X^{(i)}|F^{(j)}] = X^{(i)}$  for  $i \leq j$  and a sequence of random variables  $\{X^{(i)}\}_i$  [39]. Although the elements of  $F^{(j)}$  are events, identifying one element of  $F^{(j)}$  is equivalent to identifying the first  $j$  measurement outcomes. Therefore,  $E[X^{(i)}|F^{(j)}]$  is regarded as the expectation of  $X^{(i)}$  conditioned on the first  $j$  measurement outcomes. Then, the conditional expectations of random variables  $\chi_{\text{ph}}^{(i)}$ ,  $\chi_a^{(i)}$ , and  $\chi_{\text{bit}}^{(i)}$  are, respectively, given by

$$E[\chi_{\text{ph}}^{(i)}|F^{(i-1)}] = t \cdot \text{tr}[\hat{e}_{\text{ph}} \hat{\sigma}_{AB}^{F^{(i-1)}}], \quad (35)$$

$$E[\chi_a^{(i)}|F^{(i-1)}] = t \cdot \text{tr}[\hat{P}_a \hat{\sigma}_{AB}^{F^{(i-1)}}], \quad (36)$$

$$E[\chi_{\text{bit}}^{(i)}|F^{(i-1)}] = (1 - t) \cdot \text{tr}[\hat{e}_{\text{bit}} \hat{\sigma}_{AB}^{F^{(i-1)}}]. \quad (37)$$

Here,  $\hat{\sigma}_{AB}^{F^{(i-1)}}$  denotes the state of systems  $AB$  conditional on the first  $(i - 1)$  measurement outcomes. Since Eq. (30) holds for any state  $\hat{\sigma}_{AB}$ , Eq. (30) can be rewritten by using the

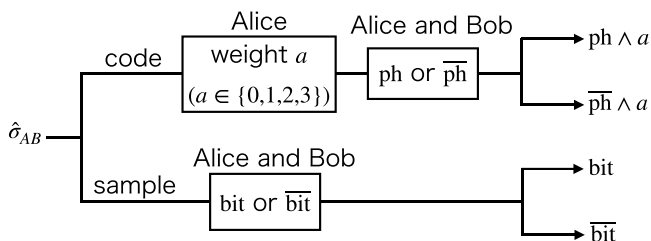


FIG. 3. This figure illustrates the measurements performed by Alice and Bob in the code and sample rounds, respectively.

conditional expectations as

$$\begin{aligned} & \frac{E[\chi_{\text{ph}}^{(i)}|F^{(i-1)}]}{t} - \frac{\lambda}{1-t} E[\chi_{\text{bit}}^{(i)}|F^{(i-1)}] - \sum_{a=2,3} \frac{E[\chi_a^{(i)}|F^{(i-1)}]}{t} \\ & \leq \frac{\lambda}{t} \sqrt{E[\chi_1^{(i)}|F^{(i-1)}] \cdot E[\chi_3^{(i)}|F^{(i-1)}]}. \end{aligned} \quad (38)$$

Taking the sum of the conditional expectations over all the detected events and using the Cauchy-Schwartz inequality lead to

$$\begin{aligned} & \sum_{i=1}^{N_{\text{det}}} \left( \frac{1}{t} E[\chi_{\text{ph}}^{(i)}|F^{(i-1)}] - \frac{\lambda}{1-t} E[\chi_{\text{bit}}^{(i)}|F^{(i-1)}] \right. \\ & \quad \left. - \frac{1}{t} \sum_{a=2,3} E[\chi_a^{(i)}|F^{(i-1)}] \right) \\ & \leq \frac{\lambda}{t} \sqrt{\left( \sum_{i=1}^{N_{\text{det}}} E[\chi_1^{(i)}|F^{(i-1)}] \right) \left( \sum_{i=1}^{N_{\text{det}}} E[\chi_3^{(i)}|F^{(i-1)}] \right)}. \end{aligned} \quad (39)$$

Next, we transform this inequality into the one in terms of the random variables  $\sum_{i=1}^{N_{\text{det}}} \chi_{\text{ph}}^{(i)}$ ,  $\sum_{i=1}^{N_{\text{det}}} \chi_{\text{bit}}^{(i)}$ , and  $\sum_{i=1}^{N_{\text{det}}} \chi_a^{(i)}$ . In so doing, we exploit two concentration inequalities, Azuma’s [27] and Kato’s inequalities [32], which can be applied to correlated random variables. Azuma’s inequality is a typical technique to bound the sum of conditional expectations with the number of occurrences and is widely used in the security proofs of QKD [21,22,28–31]. The explicit statement of this inequality is shown in Appendix D 1. The deviation term of Azuma’s inequality scales with  $\sqrt{N_{\text{det}}}$ , which is independent of the magnitude of the target sum of conditional expectations. Hence, if this target sum is comparable to the deviation term, Azuma’s inequality gives a reasonably tight bound. Unfortunately, however, if this sum is much smaller than the number of trials, this inequality only provides a loose bound. In our analysis, this is the case when we bound the following sum of conditional expectations:

$$S_3 := \sum_{i=1}^{N_{\text{det}}} E[\chi_3^{(i)}|F^{(i-1)}], \quad (40)$$

with random variable  $N_3 := \sum_{i=1}^{N_{\text{det}}} \chi_3^{(i)}$ . The number of the weight being three (namely,  $a = 3$ ) implies that the state of a single block contains at least three photons [40], whose probability of occurrence is much smaller than one. This means that  $S_3$  is generally much smaller than  $N_{\text{det}}$ , and hence Azuma’s inequality only provides a loose bound on  $S_3$ .

On the other hand, Kato’s inequality is the recently found concentration inequality that always gives a tighter bound than Azuma’s inequality and is employed in recent finite-key analyses [20,41–43]. Kato’s inequality has a significant advantage over Azuma’s one, especially when the target sum of conditional expectations is much smaller than the number of trials. This advantage is brought by incorporating our prediction  $N_3^*$  of  $N_3$  into the estimation of  $S_3$ . The accuracy of this prediction only affects the tightness of this inequality, which is tightest when  $N_3^* = N_3$ , and the inequality is still valid even if the prediction fails. In our security analysis, we found that Kato’s inequality indeed improves the key rate by

tightly estimating  $S_3$  for which Azuma's inequality is not tight. On the other hand, Azuma's inequality is sufficiently tight for all the other components whose conditional expectations are larger. For instance, in estimating the following sum of conditional expectations:

$$S_2 := \sum_{i=1}^{N_{\text{det}}} \sum_{a=2,3} E[\chi_a^{(i)} | F^{(i-1)}], \quad (41)$$

Azuma's inequality gives a tight bound because  $S_2$  is generally much larger than  $S_3$ . As a result, we confirm that the probability of multiple photon emission events, in which two or more than two photons are emitted, is not small enough to benefit significantly from Kato's inequality. This result implies that the finite-key analysis of the BB84 protocol with nonphase randomized light sources could not be drastically improved by applying Kato's inequality instead of Azuma's because the number of phase errors is given by the numbers of bit errors

and essentially the multiple photon emission events [44]. On the other hand, the key rate of the twin-field protocol [20] is substantially increased by using Kato's inequality to estimate the sum of the expectations of vacuum detections. This is so because the vacuum detection occurs with about the dark count probability (such as  $10^{-8}$  assumed in Ref. [20]), and this event is rare enough to benefit significantly from this inequality. To summarize the discussion so far, Kato's inequality could drastically improve the key rate of QKD protocols if the derived number of phase errors contains the number of occurrences of very rare events, such as vacuum detection and three-photon emission events.

In Appendix D 2, we explain how to apply Kato's inequality to bound  $S_3$  with  $N_3$  and its prediction  $N_3^*$ . We leave the details of deriving the upper bound on the number of phase errors  $N_{\text{ph}}^U$  from Eq. (39) to Appendix C and just state our main result as follows.

*Theorem 3.* For the protocol described in Sec. III, the number of phase errors satisfies

$$N_{\text{ph}} \leq N_{\text{ph}}^U := \frac{\lambda t e_{\text{bit}} N_{\text{samp}}}{1-t} + (tq_2 N_{\text{em}} + \Gamma_2) + \lambda \times \sqrt{[tq_1 N_{\text{em}} + \Gamma_1 + \Delta(1, \epsilon_1)] \left\{ (tq_3 N_{\text{em}} + \Gamma_3) \left( 1 + \frac{2a^*(N_{\text{det}}, N_3^*, \epsilon_1)}{\sqrt{N_{\text{det}}}} \right) + [b^*(N_{\text{det}}, N_3^*, \epsilon_1) - a^*(N_{\text{det}}, N_3^*, \epsilon_1)] \sqrt{N_{\text{det}}} \right\} + t\Delta(D^2, \epsilon_1)}, \quad (42)$$

except for probability  $3\epsilon_1 + 3\epsilon_2$ , with  $\epsilon_1$  and  $\epsilon_2$  being the failure probabilities of the parameter estimation steps. Here,

$$\Delta(x, y) := \sqrt{2xN_{\text{det}} \ln \frac{1}{y}}, \quad (43)$$

$$\lambda := 3 + \sqrt{5}, \quad (44)$$

$$\Gamma_n := \frac{1}{2}[-\ln \epsilon_2 + \sqrt{(\ln \epsilon_2)^2 - 8tq_n N_{\text{em}} \ln \epsilon_2}], \quad (45)$$

$$N_3^* = \min \{ tq_3 N_{\text{em}} + \Gamma_3, \lfloor (N_{\text{det}} - 1)/2 \rfloor \}, \quad (46)$$

$$D := \max \left\{ \frac{\lambda}{1-t} + 1, \frac{1}{t} + \lambda + 1 \right\}, \quad (47)$$

$$a^*(n, m, \epsilon) := \max \left\{ -\frac{\sqrt{n}}{2}, \frac{216\sqrt{nm}(n-m) \ln \epsilon - 48n^{\frac{3}{2}}(\ln \epsilon)^2 + 27\sqrt{2}(n-2m)\sqrt{-n^2(\ln \epsilon)[9m(n-m) - 2n \ln \epsilon]}}{4(9n - 8 \ln \epsilon)[9m(n-m) - 2n \ln \epsilon]} \right\} \quad (48)$$

$$b^*(n, m, \epsilon) := \frac{\sqrt{18a^*(n, m, \epsilon)^2 n - [16a^*(n, m, \epsilon)^2 + 24a^*(n, m, \epsilon)\sqrt{n} + 9n] \ln \epsilon}}{3\sqrt{2n}}. \quad (49)$$

Recall that probability  $q_n$  is defined in Eq. (3).

With this theorem, we complete the derivation of Eq. (21) and our security proof.

## V. SIMULATIONS OF KEY RATES

In this section, we present the simulation results of the key rate  $R := \ell/3N_{\text{em}}$  of our DPS protocol as a function of the channel transmission  $\eta$  including the detection efficiency.

From Corollary 1 and Theorem 3,  $\ell$  can be expressed as

$$\ell = N_{\text{code}} [1 - h(N_{\text{ph}}^U/N_{\text{code}})] - \zeta - N_{\text{EC}} - \zeta', \quad (50)$$

with  $\epsilon_{\text{sec}} = 2^{-\zeta'} + \sqrt{2}\sqrt{3\epsilon_1 + 3\epsilon_2 + 2^{-\zeta}}$  secure. For our simulation, we suppose that each emitted pulse is a coherent pulse from a laser with the mean photon number  $\mu$ . In this case,  $q_a$

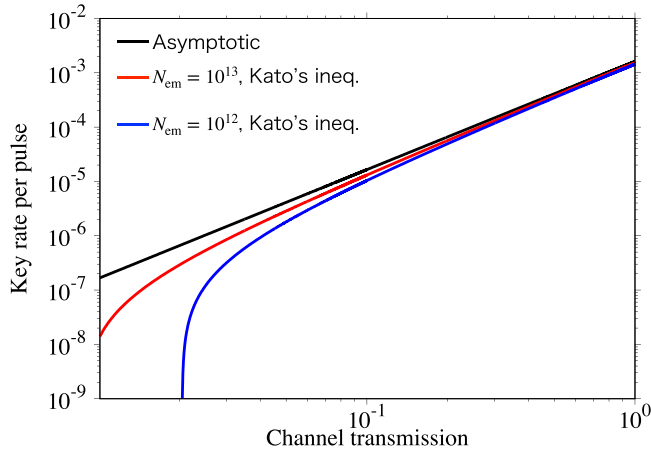


FIG. 4. Secure key rate  $R$  per a single emitted pulse as a function of the overall channel transmission  $\eta$ . From bottom to top, we plot the key rates for  $N_{\text{em}} = 10^{12}$ ,  $10^{13}$ , and the asymptotic case under the bit error rate of  $e_{\text{bit}} = 1\%$  and the security parameter of  $\epsilon_{\text{sec}} \doteq 10^{-8.1}$ .

defined in Eq. (3) is written as

$$q_a = \sum_{v=a}^{\infty} e^{-3\mu} (3\mu)^v / v!. \quad (51)$$

We assume the number of detected rounds as

$$\begin{aligned} N_{\text{det}} &= N_{\text{em}} \times 2\eta\mu e^{-2\eta\mu}, \\ N_{\text{code}} &= tN_{\text{det}}, \\ N_{\text{samp}} &= (1-t)N_{\text{det}}, \end{aligned} \quad (52)$$

and the practical cost of error correction being  $N_{\text{EC}} = 1.16N_{\text{code}}h(e_{\text{bit}})$  with 1.16 [45] is an error correction inefficiency. Also, we set  $\zeta' = 28$ ,  $\zeta = 58$ , and  $\epsilon_1 = \epsilon_2 = 2^{-58}/6$ , which results in  $\epsilon_{\text{sec}} = 2^{-27} \doteq 10^{-8.1}$ . The key rate  $R$  is optimized over the mean photon number  $\mu$  and the probability  $t$  of choosing the code round in step (P2) for each value of  $\eta$ . The results are shown in Fig. 4. The optimal mean photon number  $\mu_{\text{opt}}$  against the channel transmission  $\eta$  when  $N_{\text{em}} = 10^{13}$  is  $(\eta, \mu_{\text{opt}}) = (1, 9.3 \times 10^{-3})$ ,  $(0.1, 9.4 \times 10^{-4})$ ,  $(0.01, 9.0 \times 10^{-5})$ . From the result with  $N_{\text{em}} = 10^{13}$  in Fig. 4, if we assume the overall channel transmission as  $\eta = 0.5 \times 10^{-0.2l/10}$  with  $l$  denoting the distance between Alice and Bob and laser diodes operating at 1 GHz repetition rate, by running our protocol for 8.3 hours, we can generate a 3 Mbit secret key for a channel length of 77 km under the bit error rate of 1%.

## VI. COMPARISONS OF KEY RATES WITH AZUMA'S AND KATO'S INEQUALITIES

As explained in Sec. IV C, we apply Kato's inequality to upper-bound  $S_3$  in Eq. (40). We remark that the security proof is valid even if we instead use Azuma's inequality to bound  $S_3$ , and in this case, the final expression of  $N_{\text{ph}}^{\text{U}}$  in Eq. (42) is

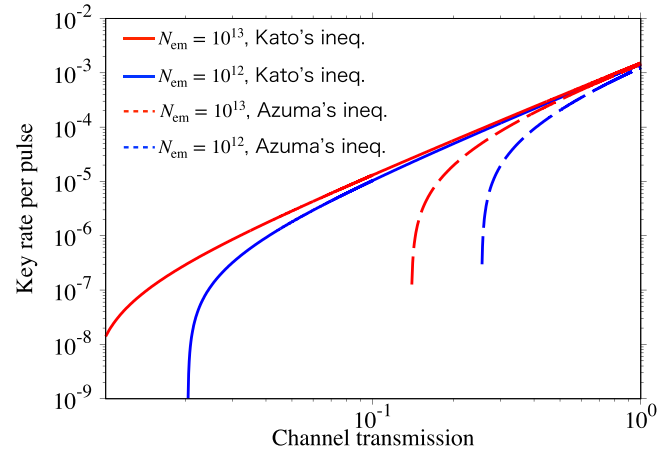


FIG. 5. Secure key rate  $R$  per a single emitted pulse as a function of the overall channel transmission  $\eta$ . The top two curves are the key rates for  $N_{\text{em}} = 10^{13}$  and  $10^{12}$  under  $e_{\text{bit}} = 1\%$  and  $\epsilon_{\text{sec}} \doteq 10^{-8.1}$  when Kato's inequality is used in the security proof (these two curves are the same as the two bottom curves in Fig. 4). The two bottom dashed curves in this figure are the key rates for  $N_{\text{em}} = 10^{12}$  and  $10^{13}$  from bottom to top under  $e_{\text{bit}} = 1\%$  and  $\epsilon_{\text{sec}} \doteq 10^{-8.1}$  when Azuma's inequality is used instead of Kato's one. We see that Azuma's inequality gives a slow convergence of the key rate in the finite-size regime, whose reason is discussed in Sec. VI.

replaced with

$$\begin{aligned} N_{\text{ph}}^{\text{U}} &= \frac{\lambda t e_{\text{bit}} N_{\text{samp}}}{1-t} + (tq_2 N_{\text{em}} + \Gamma_2) + \lambda t N_{\text{em}} \\ &\times \sqrt{\left[ q_1 + \frac{\Gamma_1 + \Delta(1, \epsilon_1)}{tN_{\text{em}}} \right] \left[ q_3 + \frac{\Gamma_3 + \Delta(1, \epsilon_1)}{tN_{\text{em}}} \right]} \\ &+ t\Delta(F^2, \epsilon_1). \end{aligned} \quad (53)$$

To see how much the key rate degrades if we instead use this bound for the simulation of the key rate, we compare the key rate based on the bound in Eq. (42) with the one based on Eq. (53) in Fig. 5. From this figure, it is clear that Kato's inequality gives a substantially better key rate in the finite-size regime. The slow convergence of the key rate using Azuma's inequality is due to the deviation term  $\Delta(1, \epsilon_1)/tN_{\text{em}}$  in  $q_3 + \frac{\Gamma_3 + \Delta(1, \epsilon_1)}{tN_{\text{em}}}$ . Here,  $q_3$  in Eq. (51) is in the order of  $O(\mu^3) \sim O(\eta^3)$ , and the deviation term is in the order of

$$\frac{\Delta(1, \epsilon_1)}{tN_{\text{em}}} = \frac{1}{t} \sqrt{\frac{2 \ln \frac{1}{\epsilon_1}}{N_{\text{em}}}} \sqrt{Q} = O(\sqrt{Q}) = O(\sqrt{\eta\mu}) = O(\eta), \quad (54)$$

since  $\mu = O(\eta)$ . We illustrate in Fig. 6 the comparison of  $q_3$  and  $\Delta(1, \epsilon_1)/tN_{\text{em}}$ , and the asymptotic key rate and the finite one using Azuma's inequality. From this figure, we see that the two lines of  $q_3 \sim O(\eta^3)$  and  $\Delta(1, \epsilon_1)/tN_{\text{em}} \sim O(\eta)$  intersect at  $\eta \doteq 0.29$ , and the deviation term becomes dominant when  $\eta < 0.29$ . This is the reason for drastically increasing the divergence of the two key rates after the point of  $\eta = 0.29$ .

Note that from Ref. [32], when we increase the intensity and three photons are more likely to be emitted, the difference in the deviation terms of Kato's and Azuma's inequalities becomes smaller. Hence, one may expect that the difference



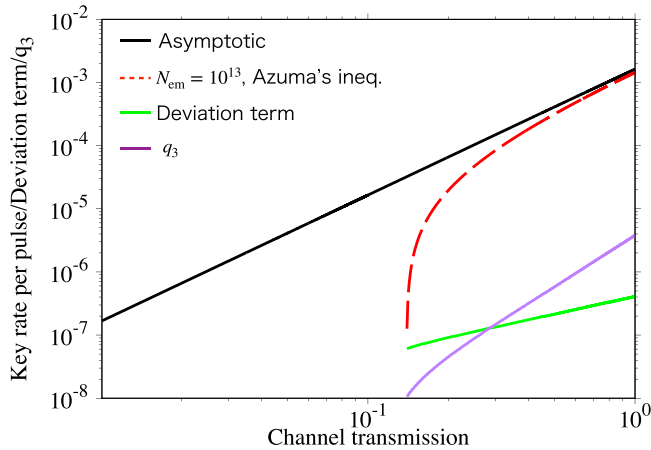


FIG. 6. This figure illustrates why Azuma’s inequality results in slow convergence of the key rate. The top black line is the asymptotic key rate (same as the black line in Fig. 4) and the second top curve is the one with  $N_{em} = 10^{13}$  when Azuma’s inequality is used (same as the red dashed curve in Fig. 5). The bottom purple and green lines represent  $q_3$  and the deviation term  $\Delta(1, \epsilon_1)/tN_{em}$  of Azuma’s inequality with  $N_{em} = 10^{13}$ , respectively. The green and purple lines intersect at about  $\eta = 0.29$ , and after this point the deviation term becomes dominant and the divergence of the two key rates increases drastically.

in the key rates under these two inequalities also becomes smaller by increasing the intensity. However, we do not observe such a tendency. This implies that the improvement we would obtain by increasing the intensities to decrease the deviations terms is overwhelmed by the use of nonoptimal intensities.

VII. CONCLUSIONS

This paper has provided the information-theoretic security proof of the DPS QKD protocol in the finite-size regime. The main analytical result is Theorem 3, which shows the upper bound on the number of phase errors in the finite-size regime. For better performance, our analysis employs Kato’s inequality [32] to upper bound the sum of conditional expectations regarding the three-photon emission events. If we use Azuma’s inequality [27] instead of Kato’s one, the key rate is significantly degraded. This is because the deviation term of Azuma’s inequality scales with the square root of the number of trials, and hence if the sum of conditional expectations is much smaller than the number of trials, which is the case for three-photon emission events, this inequality only gives a loose bound. Fortunately, however, we have revealed that Kato’s inequality gives a much tighter deviation term than Azuma’s for these three-photon emission events and the key

rate is drastically improved. As a result of our security analysis, our numerical simulation in Fig. 4 has shown that Alice and Bob can generate a 3 Mbit secret key over 77 km for 8.3 hours under typical experimental parameters. Therefore, our results strongly suggest the feasibility of the DPS QKD under a realistic experimental setup.

We end with some open questions. In practical situations, it could be difficult for the assumption (A2) to be satisfied, which requires that the vacuum emission probabilities are the same between both bit values. This issue was already solved in Ref. [18], only in the asymptotic regime. Hence, it has of practical importance to reveal how the difference in these vacuum probabilities affects the key rate in the finite-size regime.

*Note added.* Recently, we became aware of the independent related work [46] that provides a finite-key security analysis of the DPS protocol using the entropy accumulation technique [47]. This proof is valid against the most general attacks, but requires the relativistic constraint to satisfy the sequential assumption, where Alice must wait to emit the  $(i + 1)$ th pulse until she can be sure that the  $(i + 1)$ th pulse will not affect Bob’s  $i$ th measurement outcome. For instance, this can be realized by Alice sending the  $(i + 1)$ th pulse after Bob completes the measurement of the  $i$ th pulse. The key rate per pulse  $R$  of Ref. [46] is in the order of  $O(\eta)$  while our key rate is  $R = O(\eta^2)$ , with  $\eta$  denoting the channel transmission. Importantly, however, our proof is free from such a relativistic constraint, which implies that our protocol can increase the repetition rate of the protocol as much as possible. Hence, even if our key rate per pulse is inferior to that in Ref. [46], our key rate *per second* could exceed the one of Ref. [46] in some distance regime. Regarding the device models assumed in the security proofs, our proof holds even under the existence of source imperfections but assumes the PNR detectors, while the proof in Ref. [46] assumes ideal coherent states but holds with the threshold detectors. We summarize in Table I the differences between our proof and the one in Ref. [46].

ACKNOWLEDGMENTS

We thank Hiroki Takesue, Toshimori Honjo, Koji Azuma, Takuya Ikuta, Hsin-Pin Lo, and Guillermo Currás-Lorenzo for helpful discussions. A.M. is supported by JST, ACT-X Grant No. JPMJAX2100, Japan. Y.T. is supported by the MEXT Quantum Leap Flagship Program (MEXT Q-LEAP) Grants No. JPMXS0118067394 and No. JPMXS0120319794, JST [Moonshot R&D–MILLENNIA Program] Grant No. JPMJMS2061, and the Grant-in-Aid for Scientific Research (A) No. JP22H00522 of JSPS. K.T. acknowledges support from JSPS KAKENHI Grant No. JP18H05237.

TABLE I. Comparison of our finite-key security analysis and the one in Ref. [46].

	Eve’s attack	Key rate per pulse	Sources	Detectors
Our proof	Unconditional	$O(\eta^2)$	Any source satisfying (A1)-(A3)	PNR detectors
Ref. [46]	Relativistic constraint	$O(\eta)$	Coherent states $\{ \pm \alpha\rangle\}$	Threshold detectors

**APPENDIX A: PROOF OF EQ. (16)**

In this Appendix, we prove Eq. (16). For this, we introduce the intermediate state

$$\hat{\sigma}_{ABE|N_{\text{fin}}} := \sum_{k_A, k_B} \Pr[k_A, k_B|N_{\text{fin}}] |k_A, k_A\rangle \langle k_A, k_A|_{AB} \otimes \hat{\rho}_{E|N_{\text{fin}}}^{\text{fin}}(k_A, k_B), \tag{A1}$$

and the triangle inequality of the 1-norm gives

$$\|\hat{\rho}_{ABE|N_{\text{fin}}}^{\text{ideal}} - \hat{\rho}_{ABE|N_{\text{fin}}}^{\text{fin}}\|_1 \leq \|\hat{\rho}_{ABE|N_{\text{fin}}}^{\text{ideal}} - \hat{\sigma}_{ABE|N_{\text{fin}}}\|_1 + \|\hat{\sigma}_{ABE|N_{\text{fin}}} - \hat{\rho}_{ABE|N_{\text{fin}}}^{\text{fin}}\|_1. \tag{A2}$$

We first calculate the first term as follows:

$$\begin{aligned} & \|\hat{\rho}_{ABE|N_{\text{fin}}}^{\text{ideal}} - \hat{\sigma}_{ABE|N_{\text{fin}}}\|_1 \\ &= \left\| \frac{1}{2^{N_{\text{fin}}}} \sum_k |k, k\rangle \langle k, k|_{AB} \otimes \text{tr}_{AB}(\hat{\rho}_{ABE|N_{\text{fin}}}^{\text{fin}}) - \sum_{k_A, k_B} \Pr[k_A, k_B|N_{\text{fin}}] |k_A, k_A\rangle \langle k_A, k_A|_{AB} \otimes \hat{\rho}_{E|N_{\text{fin}}}^{\text{fin}}(k_A, k_B) \right\|_1 \end{aligned} \tag{A3}$$

$$= \left\| \hat{U} \left[ \frac{1}{2^{N_{\text{fin}}}} \sum_k |k, k\rangle \langle k, k|_{AB} \otimes \text{tr}_{AB}(\hat{\rho}_{ABE|N_{\text{fin}}}^{\text{fin}}) - \sum_{k_A, k_B} \Pr[k_A, k_B|N_{\text{fin}}] |k_A, k_A\rangle \langle k_A, k_A|_{AB} \otimes \hat{\rho}_{E|N_{\text{fin}}}^{\text{fin}}(k_A, k_B) \right] \hat{U}^\dagger \right\|_1 \tag{A4}$$

$$= \left\| \frac{1}{2^{N_{\text{fin}}}} \sum_k |k\rangle \langle k|_A \otimes \text{tr}_{AB}(\hat{\rho}_{ABE|N_{\text{fin}}}^{\text{fin}}) - \sum_{k_A, k_B} \Pr[k_A, k_B|N_{\text{fin}}] |k_A\rangle \langle k_A|_A \otimes \hat{\rho}_{E|N_{\text{fin}}}^{\text{fin}}(k_A, k_B) \right\|_1 \tag{A5}$$

$$= \|\hat{\rho}_{AE|N_{\text{fin}}}^{\text{ideal}} - \hat{\rho}_{AE|N_{\text{fin}}}^{\text{fin}}\|_1. \tag{A6}$$

We obtain the first equality by substituting the definitions in Eqs. (10) and (A1). The second equality follows from the unitary-invariance property of the 1-norm. The third equality follows by setting the unitary operator as  $\hat{U} = \sum_k |k\rangle \langle k|_A \otimes \bigotimes_{i=1}^{N_{\text{fin}}} \hat{X}_{B_i}^{k_i}$  with  $\hat{X}_B$  denoting the Pauli- $X$  operator acting on system  $B$ . The final equality follows by the definitions in Eqs. (14) and (15). Combining Eqs. (13) and (A6) results in

$$\frac{1}{2} \sum_{N_{\text{fin}} \geq 0} \Pr[N_{\text{fin}}] \|\hat{\rho}_{ABE|N_{\text{fin}}}^{\text{ideal}} - \hat{\sigma}_{ABE|N_{\text{fin}}}\|_1 \leq \epsilon_s. \tag{A7}$$

Next, we calculate the second term of Eq. (A2) as follows:

$$\|\hat{\sigma}_{ABE|N_{\text{fin}}} - \hat{\rho}_{ABE|N_{\text{fin}}}^{\text{fin}}\|_1 = \left\| \sum_{k_A, k_B} \Pr[k_A, k_B|N_{\text{fin}}] (\hat{P}[|k_A, k_A\rangle_{AB}] - \hat{P}[|k_A, k_B\rangle_{AB}]) \otimes \hat{\rho}_{E|N_{\text{fin}}}^{\text{fin}}(k_A, k_B) \right\|_1 \tag{A8}$$

$$= \left\| \sum_{\substack{k_A, k_B \\ k_A \neq k_B}} \Pr[k_A, k_B|N_{\text{fin}}] (\hat{P}[|k_A, k_A\rangle_{AB}] - \hat{P}[|k_A, k_B\rangle_{AB}]) \otimes \hat{\rho}_{E|N_{\text{fin}}}^{\text{fin}}(k_A, k_B) \right\|_1 \tag{A9}$$

$$\begin{aligned} &= \left\| \sum_{\substack{k_A, k_B \\ k_A \neq k_B}} \Pr[k_A, k_B|N_{\text{fin}}] \hat{P}[|k_A, k_A\rangle] \otimes \hat{\rho}_{E|N_{\text{fin}}}^{\text{fin}}(k_A, k_B) \right\|_1 \\ &+ \left\| \sum_{\substack{k_A, k_B \\ k_A \neq k_B}} \Pr[k_A, k_B|N_{\text{fin}}] \hat{P}[|k_A, k_B\rangle] \otimes \hat{\rho}_{E|N_{\text{fin}}}^{\text{fin}}(k_A, k_B) \right\|_1 \end{aligned} \tag{A10}$$

$$= \sum_{k_A, k_B: k_A \neq k_B} \Pr[k_A, k_B|N_{\text{fin}}] + \sum_{k_A, k_B: k_A \neq k_B} \Pr[k_A, k_B|N_{\text{fin}}] = 2\Pr[k_A \neq k_B|N_{\text{fin}}]. \tag{A11}$$

We obtain the first equality by substituting the definitions in Eqs. (A1) and (9). The third equality follows from  $\langle k_A, k_B | k_A, k_A \rangle = 0$  with  $k_A \neq k_B$ . The fourth equality follows by  $\|\hat{A}\|_1 = \text{tr}(\hat{A})$  for  $\hat{A} \geq 0$ . From Eqs. (12) and (A11), we have

$$\frac{1}{2} \sum_{N_{\text{fin}} \geq 0} \Pr[N_{\text{fin}}] \|\hat{\sigma}_{ABE|N_{\text{fin}}} - \hat{\rho}_{ABE|N_{\text{fin}}}^{\text{fin}}\|_1 \leq \epsilon_c. \quad (\text{A12})$$

Combining Eqs. (A2), (A7), and (A12) results in Eq. (16), which ends the proof of Eq. (16).  $\blacksquare$

### APPENDIX B: PROOF OF THEOREM 1

In this Appendix, we prove Theorem 1. This theorem can be obtained by calculating the left-hand side of Eq. (12) as

$$\Pr[k_A \neq k_B \wedge N_{\text{fin}} \geq 0] = \Pr[k_A \neq k_B \wedge N_{\text{fin}} \geq 1] \quad (\text{B1})$$

$$\leq \Pr[k_A \neq k_B \wedge H_{\text{EC}}(\kappa_A) = H_{\text{EC}}(\kappa_B^{\text{rec}})] \quad (\text{B2})$$

$$\leq \Pr[\kappa_A \neq \kappa_B^{\text{rec}} \wedge H_{\text{EC}}(\kappa_A) = H_{\text{EC}}(\kappa_B^{\text{rec}})] \quad (\text{B3})$$

$$= \Pr[\kappa_A \neq \kappa_B^{\text{rec}}] \cdot \Pr[H_{\text{EC}}(\kappa_A) = H_{\text{EC}}(\kappa_B^{\text{rec}}) | \kappa_A \neq \kappa_B^{\text{rec}}] \quad (\text{B4})$$

$$\leq \Pr[H_{\text{EC}}(\kappa_A) = H_{\text{EC}}(\kappa_B^{\text{rec}}) | \kappa_A \neq \kappa_B^{\text{rec}}] \quad (\text{B5})$$

$$\leq 2^{-\zeta'}. \quad (\text{B6})$$

The first equality follows from  $\Pr[k_A \neq k_B | N_{\text{fin}} = 0] = 0$ . The first inequality follows because  $H_{\text{EC}}(\kappa_A) = H_{\text{EC}}(\kappa_B^{\text{rec}})$  is a necessary condition of  $N_{\text{fin}} \geq 1$ . Recall that  $H_{\text{EC}}$  is the universal<sub>2</sub> hash function used in verification of error correction at step (P5). The second inequality follows because  $k_A \neq k_B$  leads to  $\kappa_A \neq \kappa_B^{\text{rec}}$ . The last inequality is due to the definition of the universal<sub>2</sub> hash function, namely,  $\Pr[H_{\text{EC}}(x) = H_{\text{EC}}(x')] \leq \frac{1}{|\mathcal{Y}|}$  holds for any pair of distinct elements  $x, x' \in \mathcal{X}$  when the universal<sub>2</sub> hash function  $H_{\text{EC}} : \mathcal{X} \rightarrow \mathcal{Y}$  is chosen uniformly at random.  $\blacksquare$

### APPENDIX C: PROOF OF THEOREM 3

In this Appendix, we prove our main result, Theorem 3, by executing statistical analysis using Azuma's and Kato's inequalities and the Chernoff bound. To derive this theorem from Eq. (39), we first employ Azuma's inequality (see Appendix D 1 for details). In so doing, we define the following random variable:

$$X^{(i)} := \sum_{p=1}^i \left[ \frac{1}{t} (\chi_{\text{ph}}^{(p)} - E[\chi_{\text{ph}}^{(p)} | F^{(p-1)}]) - \frac{\lambda}{1-t} (\chi_{\text{bit}}^{(p)} - E[\chi_{\text{bit}}^{(p)} | F^{(p-1)}]) - \frac{1}{t} \sum_{a=2,3} (\chi_a^{(p)} - E[\chi_a^{(p)} | F^{(p-1)}]) \right]. \quad (\text{C1})$$

Since  $X^{(i-1)}$  becomes constant given  $F^{(i-1)}$ , the sequence of random variables  $\{X^{(i)}\}_{i=0}^{N_{\text{det}}}$  with  $X^{(0)} = 0$  satisfies the martingale condition defined in Eq. (D1), namely,  $E[X^{(i)} | F^{(i-1)}] - X^{(i-1)} = E[X^{(i)} - X^{(i-1)} | F^{(i-1)}] = 0$ . Next, we derive the bounded difference parameter  $D$  in Eq. (D2). Substituting Eq. (C1) to  $|X^{(i)} - X^{(i-1)}|$  and using Eqs. (35)–(37) leads to

$$|X^{(i)} - X^{(i-1)}| = \left| \frac{1}{t} \chi_{\text{ph}}^{(i)} - \text{tr}[\hat{\rho}_{\text{ph}} \hat{\sigma}_{AB}^{F^{(i-1)}}] - \frac{\lambda}{1-t} \chi_{\text{bit}}^{(i)} + \lambda \cdot \text{tr}[\hat{\rho}_{\text{bit}} \hat{\sigma}_{AB}^{F^{(i-1)}}] - \sum_{a=2,3} \left( \frac{1}{t} \chi_a^{(i)} - \text{tr}[\hat{\rho}_a \hat{\sigma}_{AB}^{F^{(i-1)}}] \right) \right|. \quad (\text{C2})$$

If the  $i$ th detected round is the sample one, Alice and Bob measure their systems to learn whether a bit error occurs or not (Fig. 3 depicts the measurement in the sample round). In this case, a possible measurement outcome is in  $\{\text{bit}, \overline{\text{bit}}\}$ , and hence we have  $|X^{(i)} - X^{(i-1)}| \leq \frac{\lambda}{1-t} + 1$ . Here, we use  $|a - b| \leq \max\{a, b\}$  for any  $a, b \geq 0$ . On the other hand, if the  $i$ th detected round is the code one, Alice learns weight  $a$ , and Alice and Bob measure their systems to learn whether a phase error occurs or not (Fig. 3 depicts the measurement in the code round). In this case, a possible measurement outcome is in  $\bigcup_{a=0}^3 \{\text{ph} \wedge a, \overline{\text{ph}} \wedge a\}$ , and hence we have  $|X^{(i)} - X^{(i-1)}| \leq \frac{1}{t} + \lambda + 1$ , where we again use  $|a - b| \leq \max\{a, b\}$  for any  $a, b \geq 0$ . By defining

$$D := \max \left\{ \frac{\lambda}{1-t} + 1, \frac{1}{t} + \lambda + 1 \right\}, \quad (\text{C3})$$

Azuma's inequality in Eq. (D3) leads to

$$\Pr \left[ X^{(N_{\text{det}})} \geq \sqrt{2N_{\text{det}} D^2 \ln \frac{1}{\epsilon_1}} \right] \leq \epsilon_1. \quad (\text{C4})$$

This results in

$$\frac{1}{t} N_{\text{ph}} - \frac{\lambda}{1-t} N_{\text{bit}} - \frac{1}{t} N_{a \geq 2} \leq \sum_{i=1}^{N_{\text{det}}} \left( \frac{1}{t} E[\chi_{\text{ph}}^{(i)} | F^{(i-1)}] - \frac{\lambda}{1-t} E[\chi_{\text{bit}}^{(i)} | F^{(i-1)}] - \frac{1}{t} \sum_{a=2,3} E[\chi_a^{(i)} | F^{(i-1)}] \right) + \Delta(D^2, \epsilon_1), \quad (\text{C5})$$

which holds except for probability  $\epsilon_1$ . Here, we define

$$N_{\text{ph}} := \sum_{i=1}^{N_{\text{det}}} \chi_{\text{ph}}^{(i)}, \quad N_{\text{bit}} := \sum_{i=1}^{N_{\text{det}}} \chi_{\text{bit}}^{(i)}, \quad N_a := \sum_{i=1}^{N_{\text{det}}} \chi_a^{(i)}, \quad N_{a \geq m} := \sum_{a'=m}^3 N_{a=a'}. \quad (\text{C6})$$

Applying Eq. (39) to Eq. (C5) gives

$$\Pr \left[ \frac{1}{t} N_{\text{ph}} - \frac{\lambda}{1-t} N_{\text{bit}} - \frac{1}{t} N_{a \geq 2} \leq \frac{\lambda}{t} \sqrt{\left( \sum_{i=1}^{N_{\text{det}}} E[\chi_1^{(i)} | F^{(i-1)}] \right) \left( \sum_{i=1}^{N_{\text{det}}} E[\chi_3^{(i)} | F^{(i-1)}] \right)} + \Delta(D^2, \epsilon_1) \right] \geq 1 - \epsilon_1. \quad (\text{C7})$$

In a similar way as we applied Azuma’s inequality to the random variable in Eq. (C1), we apply this inequality to the first sum of the conditional expectations in the square root. Importantly, as explained in Sec. IV C, we use Kato’s inequality (see Appendix D 2 for details) to bound the second sum of the conditional expectations. By applying Azuma’s and Kato’s inequalities to Eq. (C7), we have

$$\Pr \left[ \frac{1}{t} N_{\text{ph}} - \frac{\lambda}{1-t} N_{\text{bit}} - \frac{1}{t} N_{a \geq 2} \leq \frac{\lambda}{t} \sqrt{[N_1 + \Delta(1, \epsilon_1)] \cdot [N_3 + \Omega(N_{\text{det}}, N_3, N_3^*, \epsilon_1)]} + \Delta(D^2, \epsilon_1) \right] \geq 1 - 3\epsilon_1, \quad (\text{C8})$$

with

$$\Omega(N_{\text{det}}, N_3, N_3^*, \epsilon_1) := \left[ b^*(N_{\text{det}}, N_3^*, \epsilon_1) + a^*(N_{\text{det}}, N_3^*, \epsilon_1) \left( \frac{2N_3}{N_{\text{det}}} - 1 \right) \right] \sqrt{N_{\text{det}}}. \quad (\text{C9})$$

Here,  $a^*(N_{\text{det}}, N_3^*, \epsilon_1)$  and  $b^*(N_{\text{det}}, N_3^*, \epsilon_1)$  are defined in Eqs. (48) and (49), respectively, and recall that  $N_3^*$  denotes the prediction of  $N_3$ . Since  $[N_3 + \Omega(N_{\text{det}}, N_3, N_3^*, \epsilon_1)]$  is nondecreasing against  $N_3$ , we can exploit a trivial inclusion relation  $N_a \leq M_a$  that the number  $M_a$  of emitted blocks with weight  $a$  is no smaller than that of  $N_a$  and obtain

$$\Pr \left[ N_{\text{ph}} \leq \frac{\lambda t e_{\text{bit}} N_{\text{samp}}}{1-t} + M_{a \geq 2} + \lambda \sqrt{[M_1 + \Delta(1, \epsilon_1)][M_3 + \Omega(N_{\text{det}}, M_3, N_3^*, \epsilon_1)]} + t \Delta(D^2, \epsilon_1) \right] \geq 1 - 3\epsilon_1. \quad (\text{C10})$$

Applying the Chernoff bound, for any  $\epsilon_2$  ( $0 \leq \epsilon_2 \leq 1$ ),

$$M_{a \geq a'} \leq t q_{a'} N_{\text{em}} + \Gamma_{a'} \quad (\text{C11})$$

holds except for probability  $\epsilon_2$  with  $\Gamma_a := \frac{1}{2}[-\ln \epsilon_2 + \sqrt{(\ln \epsilon_2)^2 - 8t q_a N_{\text{em}} \ln \epsilon_2}]$ . Recall that probability  $q_a$  is defined in Eq. (3). Substituting the upper bound in Eq. (C11) to Eq. (C10), Eq. (C10) results in Eq. (42), which ends the proof of Theorem 3.

### APPENDIX D: CONCENTRATION INEQUALITIES

In this Appendix, we describe two concentration inequalities, Azuma’s and Kato’s inequalities, which are used in deriving the upper bound on the number of phase errors in Sec. IV C.

#### 1. Azuma’s inequality

*Theorem 4.* (Azuma’s inequality [27].) For  $n \in \mathbb{N}$ , let  $\{X^{(i)}\}_{i=0}^n$  be a sequence of random variables with  $X^{(0)} = 0$ , and  $\{F^{(i)}\}_{i=0}^n$  be a filtration with  $F^{(i)}$  identifying the random variables including  $\{X^{(0)}, \dots, X^{(i)}\}$ . The sequence of random variables  $\{X^{(i)}\}_{i=0}^n$  satisfies the martingale condition

$$E[X^{(i)} | F^{(i-1)}] = X^{(i-1)} \quad (\text{D1})$$

for any  $i \in \{1, \dots, n\}$ . Also, the difference sequence  $Y^{(i)} := X^{(i)} - X^{(i-1)}$  satisfies the bounded difference condition, namely, there exists a positive constant  $D > 0$  such that for any  $i \in \{1, \dots, n\}$ ,

$$|Y^{(i)}| \leq D \quad (\text{D2})$$

holds. Then, for any  $n \in \mathbb{N}$  and any  $\epsilon$  with  $0 \leq \epsilon \leq 1$ ,

$$\Pr \left[ X^{(n)} \geq \sqrt{2nD^2 \ln \frac{1}{\epsilon}} \right] \leq \epsilon. \quad (\text{D3})$$

## 2. Kato's inequality

We explain how to apply Kato's inequality [32] to derive an upper bound on  $\sum_{i=1}^{N_{\text{det}}} E[\chi_3^{(i)} | F^{(i-1)}]$  in Eq. (C7). Kato's inequality states that for any  $a \in \mathbb{R}$  and any  $b \geq |a|$ ,

$$\Pr \left[ \sum_{i=1}^{N_{\text{det}}} E[\chi_3^{(i)} | F^{(i-1)}] \geq N_3 + \left\{ b + a \left( \frac{2N_3}{N_{\text{det}}} - 1 \right) \right\} \sqrt{N_{\text{det}}} \right] \leq \exp \left[ - \frac{2b^2 - 2a^2}{\left( 1 + \frac{4a}{3\sqrt{N_{\text{det}}}} \right)^2} \right], \quad (\text{D4})$$

with  $N_3 = \sum_{i=1}^{N_{\text{det}}} \chi_3^{(i)}$ . To fix  $a$  and  $b$ , we consider minimizing the deviation term  $[b + a(\frac{2N_3}{N_{\text{det}}} - 1)]\sqrt{N_{\text{det}}}$  given the failure probability [right-hand side of Eq. (D4)] being  $\epsilon$  ( $0 \leq \epsilon \leq 1$ ). But, Alice and Bob do not know the true value of  $N_3$  even after running the protocol. Therefore, we make prediction  $N_3^*$  of  $N_3$ , and using this prediction we solve the following optimization problem:

$$\min \left[ b + a \left( \frac{2N_3^*}{N_{\text{det}}} - 1 \right) \right] \sqrt{N_{\text{det}}} \quad (\text{D5})$$

$$\text{s.t.} \quad \exp \left[ - \frac{2b^2 - 2a^2}{\left( 1 + \frac{4a}{3\sqrt{N_{\text{det}}}} \right)^2} \right] = \epsilon \quad (\text{D6})$$

$$b \geq |a|. \quad (\text{D7})$$

This problem is analytically solved in Ref. [20] as  $a'(N_{\text{det}}, N_3^*, \epsilon)$  and  $b'(N_{\text{det}}, N_3^*, \epsilon)$ , with

$$a'(n, m, \epsilon) := \frac{216\sqrt{nm}(n-m) \ln \epsilon - 48n^{\frac{3}{2}}(\ln \epsilon)^2 + 27\sqrt{2}(n-2m)\sqrt{-n^2(\ln \epsilon)[9m(n-m) - 2n \ln \epsilon]}}{4(9n - 8 \ln \epsilon)[9m(n-m) - 2n \ln \epsilon]}, \quad (\text{D8})$$

$$b'(n, m, \epsilon) := \frac{\sqrt{18a'(n, m, \epsilon)^2 n - [16a'(n, m, \epsilon)^2 + 24a'(n, m, \epsilon)\sqrt{n} + 9n] \ln \epsilon}}{3\sqrt{2n}}, \quad (\text{D9})$$

under  $N_3^* < N_{\text{det}}/2$ . These  $a'$  and  $b'$  are the optimal values of  $a$  and  $b$  when  $N_3^* = N_3$  and could be near optimal when  $N_3^*$  is close to  $N_3$ . To make  $N_3 + [b + a(\frac{2N_3}{N_{\text{det}}} - 1)]\sqrt{N_{\text{det}}}$  nondecreasing against  $N_3$ , we set  $a = a^*(N_{\text{det}}, N_3^*, \epsilon)$  and  $b = b^*(N_{\text{det}}, N_3^*, \epsilon)$  with

$$a^*(n, m, \epsilon) := \max \left\{ -\frac{\sqrt{n}}{2}, a'(n, m, \epsilon) \right\}, \quad (\text{D10})$$

$$b^*(n, m, \epsilon) := \frac{\sqrt{18a^*(n, m, \epsilon)^2 n - [16a^*(n, m, \epsilon)^2 + 24a^*(n, m, \epsilon)\sqrt{n} + 9n] \ln \epsilon}}{3\sqrt{2n}}. \quad (\text{D11})$$

Substituting  $a = a^*(N_{\text{det}}, N_3^*, \epsilon)$  and  $b = b^*(N_{\text{det}}, N_3^*, \epsilon)$  to Eq. (D4), we obtain

$$\sum_{i=1}^{N_{\text{det}}} E[\chi_3^{(i)} | F^{(i-1)}] \leq N_3 + \left[ b^*(N_{\text{det}}, N_3^*, \epsilon) + a^*(N_{\text{det}}, N_3^*, \epsilon) \left( \frac{2N_3}{N_{\text{det}}} - 1 \right) \right] \sqrt{N_{\text{det}}}. \quad (\text{D12})$$

This upper bound has a free parameter  $N_3^*$ , which is the prediction of  $N_3$  and can be freely chosen under  $N_3^* < N_{\text{det}}/2$ . For this, we set

$$N_3^* = \min \{ tq_3 N_{\text{em}} + \Gamma_3, \lfloor (N_{\text{det}} - 1)/2 \rfloor \}, \quad (\text{D13})$$

whose first element is an upper bound on  $N_3$  in Eq. (C11).

- 
- [1] C.-H. Bennett and G. Brassard, Quantum cryptography: Public key distribution and coin tossing, in Proc. IEEE Int. Conf. on Computers, Systems and Signal Processing (Bangalore, India) (IEEE, New York, 1984), pp. 175–179.
- [2] A. K. Ekert, Quantum Cryptography Based on Bell's Theorem, *Phys. Rev. Lett.* **67**, 661 (1991).
- [3] C. H. Bennett, Quantum Cryptography using any Two Nonorthogonal States, *Phys. Rev. Lett.* **68**, 3121 (1992).
- [4] D. Bruß, Optimal Eavesdropping in Quantum Cryptography with Six States, *Phys. Rev. Lett.* **81**, 3018 (1998).
- [5] V. Scarani, A. Acín, G. Ribordy, and N. Gisin, Quantum Cryptography Protocols Robust Against Photon Number Splitting Attacks for Weak Laser Pulse Implementations, *Phys. Rev. Lett.* **92**, 057901 (2004).
- [6] D. Stucki, N. Brunner, N. Gisin, V. Scarani, and H. Zbinden, Fast and simple one-way quantum key distribution, *Appl. Phys. Lett.* **87**, 194108 (2005).

- [7] K. Inoue, E. Waks, and Y. Yamamoto, Differential Phase Shift Quantum Key Distribution, *Phys. Rev. Lett.* **89**, 037902 (2002).
- [8] K. Inoue, E. Waks, and Y. Yamamoto, Differential-phase-shift quantum key distribution using coherent light, *Phys. Rev. A* **68**, 022317 (2003).
- [9] F. Grosshans and P. Grangier, Continuous Variable Quantum Cryptography using Coherent States, *Phys. Rev. Lett.* **88**, 057902 (2002).
- [10] H. Takesue, E. Diamanti, T. Honjo, C. Langrock, M. M. Fejer, K. Inoue, and Y. Yamamoto, Differential phase shift quantum key distribution experiment over 105 km fibre, *New J. Phys.* **7**, 232 (2005).
- [11] E. Diamanti, H. Takesue, C. Langrock, M. M. Fejer, and Y. Yamamoto, 100 km differential phase shift quantum key distribution experiment with low jitter up-conversion detectors, *Opt. Express* **14**, 13073 (2006).
- [12] H. Takesue, S.-W. Nam, Q. Zhang, R.-H. Hadfield, T. Honjo, K. Tamaki, and Y. Yamamoto, Quantum key distribution over a 40-dB channel loss using superconducting single-photon detectors, *Nat. Photonics* **1**, 343 (2007).
- [13] M. Sasaki, M. Fujiwara, H. Ishizuka, W. Klaus, K. Wakui, M. Takeoka, S. Miki, T. Yamashita, Z. Wang, A. Tanaka *et al.*, Field test of quantum key distribution in the Tokyo QKD Network, *Opt. Express* **19**, 10387 (2011).
- [14] K. Wen, K. Tamaki, and Y. Yamamoto, Unconditional Security of Single-Photon Differential Phase Shift Quantum Key Distribution, *Phys. Rev. Lett.* **103**, 170503 (2009).
- [15] K. Tamaki, G. Kato, and M. Koashi, Unconditional security of coherent-state-based differential phase shift quantum key distribution protocol with block-wise phase randomization, [arXiv:1208.1995v1](https://arxiv.org/abs/1208.1995v1).
- [16] A. Mizutani, T. Sasaki, G. Kato, Y. Takeuchi, and K. Tamaki, Information-theoretic security proof of differential-phase-shift quantum key distribution protocol based on complementarity, *Quantum Sci. Technol.* **3**, 014003 (2017).
- [17] A. Mizutani, T. Sasaki, Y. Takeuchi, K. Tamaki, and M. Koashi, Quantum key distribution with simply characterized light sources, *npj Quantum Inf.* **5**, 87 (2019).
- [18] A. Mizutani, Quantum key distribution with any two independent and identically distributed states, *Phys. Rev. A* **102**, 022613 (2020).
- [19] H. Endo, T. Sasaki, M. Takeoka, M. Fujiwara, M. Koashi, and M. Sasaki, Line-of-sight quantum key distribution with differential phase shift keying, *New J. Phys.* **24**, 025008 (2022).
- [20] G. Currás-Lorenzo, Á. Navarrete, K. Azuma, G. Kato, M. Curty, and M. Razavi, Tight finite-key security for twin-field quantum key distribution, *npj Quantum Inf.* **7**, 22 (2021).
- [21] A. Mizutani, M. Curty, C. C. W. Lim, N. Imoto, and K. Tamaki, Finite-key security analysis of quantum key distribution with imperfect light sources, *New J. Phys.* **17**, 093011 (2015).
- [22] A. Mizutani, G. Kato, K. Azuma, M. Curty, R. Ikuta, T. Yamamoto, N. Imoto, H.-K. Lo, and K. Tamaki, Quantum key distribution with setting-choice-independently correlated light sources, *npj Quantum Inf.* **5**, 8 (2019).
- [23] M. Curty, F. Xu, W. Cui, C. C. W. Lim, K. Tamaki, and H.-K. Lo, Finite-key analysis for measurement-device-independent quantum key distribution, *Nat. Commun.* **5**, 3732 (2014).
- [24] K. Maeda, T. Sasaki, and M. Koashi, Repeaterless quantum key distribution with efficient finite-key analysis overcoming the rate-distance limit, *Nat. Commun.* **10**, 3140 (2019).
- [25] M. Tomamichel, C. C. W. Lim, N. Gisin, and R. Renner, Tight finite-key analysis for quantum cryptography, *Nat. Commun.* **3**, 634 (2012).
- [26] M. Tomamichel and A. Leverrier, A largely self-contained and complete security proof for quantum key distribution, *Quantum* **1**, 14 (2017).
- [27] K. Azuma, Weighted sums of certain dependent random variables, *Tohoku Math. J.* **19**, 357 (1967).
- [28] J.-C. Boileau, K. Tamaki, J. Batuwantudawe, R. Laflamme, and J. M. Renes, Unconditional Security of a Three State Quantum Key Distribution Protocol, *Phys. Rev. Lett.* **94**, 040503 (2005).
- [29] S. Pironio, L. Masanes, A. Leverrier, and A. Acín, Security of Device-Independent Quantum Key Distribution in the Bounded-Quantum-Storage Model, *Phys. Rev. X* **3**, 031007 (2013).
- [30] U. Vazirani and T. Vidick, Fully Device-Independent Quantum Key Distribution, *Phys. Rev. Lett.* **113**, 140501 (2014).
- [31] K. Tamaki, H.-K. Lo, A. Mizutani, G. Kato, C. C. W. Lim, K. Azuma, and M. Curty, Security of quantum key distribution with iterative sifting, *Quantum Sci. Technol.* **3**, 014002 (2017).
- [32] G. Kato, Concentration inequality using unconfirmed knowledge, [arXiv:2002.04357v2](https://arxiv.org/abs/2002.04357v2).
- [33] J. Gu, X.-Y. Cao, Y. Fu, Z.-W. He, Z.-J. Yin, H.-L. Yin, and Z.-B. Chen, Experimental measurement-device-independent type quantum key distribution with flawed and correlated sources, *Sci. Bull.* **67**, 2167 (2022).
- [34] J. Müller-Quade and R. Renner, Composability in quantum cryptography, *New J. Phys.* **11**, 085006 (2009).
- [35] M. Koashi, Simple security proof of quantum key distribution based on complementarity, *New J. Phys.* **11**, 045018 (2009).
- [36] M. Tomamichel and R. Renner, Uncertainty Relation for Smooth Entropies, *Phys. Rev. Lett.* **106**, 110506 (2011).
- [37] M. Tomamichel, C. Schaffner, A. Smith, and R. Renner, Left-over hashing against quantum side information, *IEEE Trans. Inf. Theory* **57**, 8 (2011).
- [38] T. Matsuura, T. Sasaki, and M. Koashi, Refined security proof of the round-robin differential-phase-shift quantum key distribution and its improved performance in the finite-sized case, *Phys. Rev. A* **99**, 042303 (2019).
- [39] Note that  $F^{(0)} = \{\emptyset, \Omega\}$  and  $F^{(N_{\text{det}})} = 2^\Omega$ , and  $F^{(i)} \subseteq F^{(j)}$  with  $i \leq j$  means that the information of the measurement outcomes is updated.
- [40] Note that this statement is directly obtained from the assumptions on the light source in Sec. II A.
- [41] H. Zhou, T. Sasaki, and M. Koashi, Numerical method for finite-size security analysis of quantum key distribution, *Phys. Rev. Res.* **4**, 033126 (2022).
- [42] G. Currás-Lorenzo, Á. Navarrete, M. Pereira, and K. Tamaki, Finite-key analysis of loss-tolerant quantum key distribution based on random sampling theory, *Phys. Rev. A* **104**, 012406 (2021).
- [43] Á. Navarrete and M. Curty, Improved finite-key security analysis of quantum key distribution against Trojan-horse attacks, *Quantum Sci. Technol.* **7**, 035021 (2022).

- [44] H.-K. Lo and J. Preskill, Security of quantum key distribution using weak coherent states with nonrandom phases, *Quant. Inf. Comput.* **7**, 431 (2007).
- [45] G. Brassard and L. Salvail, Secret-key reconciliation by public discussion, in *Advances in Cryptology—EUROCRYPT '93*, edited by T. Helleseth (Springer, Berlin), pp. 410–423.
- [46] M. Sandfuchs, M. Haberland, V. Vilasini, and R. Wolf, Security of differential phase shift QKD from relativistic principles, [arXiv:2301.11340v1](https://arxiv.org/abs/2301.11340v1).
- [47] T. Metger and R. Renner, Security of quantum key distribution from generalised entropy accumulation, [arXiv:2203.04993v1](https://arxiv.org/abs/2203.04993v1).